IOPscience iopscience.iop.org

Home Search Collections Journals About Contact us My IOPscience

Correlation of the structural and electronic properties of (Ga,In)(N,As) based heterostructures

This article has been downloaded from IOPscience. Please scroll down to see the full text article.

2004 J. Phys.: Condens. Matter 16 S3053

(http://iopscience.iop.org/0953-8984/16/31/005)

View the table of contents for this issue, or go to the journal homepage for more

Download details:
IP Address: 129.252.86.83
The article was downloaded on 27/05/2010 at 16:21

Please note that terms and conditions apply.

J. Phys.: Condens. Matter **16** (2004) S3053–S3070 PII: S0953-8984(04)75674-X

Correlation of the structural and electronic properties of (Ga,In)(N,As) based heterostructures

P J Klar and K Volz

Department of Physics and Material Sciences Center, Philipps-University of Marburg, Renthof 5, D-35032 Marburg, Germany

E-mail: peter.klar@physik.uni-marburg.de and kerstin.volz@physik.uni-marburg.de

Received 2 February 2004
Published 23 July 2004
Online at stacks.iop.org/JPhysCM/16/S3053
doi:10.1088/0953-8984/16/31/005

Abstract

We give an overview of the current knowledge of the relationship between the structural and electronic properties of heterostructures containing the metastable (Ga,In)(N,As) alloy. We focus on the effects of different growth methods (i.e. molecular beam epitaxy and metal-organic vapour-phase epitaxy) and varying annealing conditions. In as-grown samples, detailed TEM studies of the morphological structural phase transition occurring in $Ga_{1-y}In_yN_xAs_{1-x}$ above a critical N content x_c as well as of interface roughness and strain fields in $Ga_{1-y}In_yN_xAs_{1-x}$/GaAs multiple quantum wells are presented. In a second part, we address the effects of thermal annealing on (Ga,In)(N,As)/GaAs quantum wells, in particular, focusing on phenomena related to the commonly observed large blueshifts of the (Ga,In)(N,As) band gap upon annealing. Extrinsic as well as intrinsic mechanisms contributing to the blueshift are described. Special attention is given to the intrinsic effect due to the rearrangement of the nearest-neighbour environment which changes from Ga-rich to In-rich during the annealing procedure. Our results suggest that by careful procedures (Ga,In)(N,As) material of high structural quality can be obtained and can be driven into a stable electronic configuration by annealing. The existence of such a stable electronic configuration and the reproducibility of the fabrication process are essential for employing metastable semiconductor alloys in devices.

1. Introduction

This paper presents an overview of the current knowledge of the correlation of structural and electronic properties of (Ga,In)(N,As)/GaAs multiple quantum well (MQW) structures. The unusual band formation process when incorporating small amounts of N into (Ga,In)As and GaAs semiconductor hosts results in a rather complex band structure of bulk (Ga,In)(N,As)

© 2004 IOP Publishing Ltd Printed in the UK

and Ga(N,As) [1–10]. Appropriate theoretical concepts for describing the band structure of these materials have currently been developed [11–26].

The quaternary material (Ga,In)(N,As) exhibits a large miscibility gap under thermodynamic equilibrium conditions [27]. Therefore, dilute nitrides are usually grown under extreme non-equilibrium conditions. Possible phase-separation effects as well as local atomic ordering due to the large miscibility gap are of great importance, as they may lead to local strains and to a deterioration of the MQW structure and hence of the optical properties. Little is also known about the incorporation behaviour of N and In, which does however have a strong influence on the structure and properties of the MQWs. Aiming for the telecommunication wavelengths at 1.3 and 1.55 μm requires compositions of around 35% In and several per cent of N, resulting in highly compressively strained material on GaAs. These compositions on GaAs substrates pose great challenges for both growth techniques, metal-organic vapour-phase epitaxy (MOVPE) and molecular beam epitaxy (MBE). On the one hand, the N solubility limit is approached and on the other hand, strain limits the maximum achievable In concentration in the QWs, both limiting the achievable wavelengths.

Furthermore, there exists a structural metastability of the quaternary alloy $Ga_{1-y}In_yN_xAs_{1-x}$ which arises due to subtle microscopic effects when both In and N are present. As one result the band gap of $Ga_{1-y}In_yN_xAs_{1-x}$ is not simply a function of composition y and x, but also depends strongly on the material history, e.g. growth conditions as well as annealing conditions. The material is usually annealed at elevated temperatures for a certain time after growth in order to enhance the photoluminescence (PL) intensity and to remove defects. There are many reports in literature on what is called ‘blueshift upon annealing’ in this material system for both growth techniques. The cause of the blue shift of the emission wavelength after annealing of the (Ga,In)(N,As) structures or even after raising the growth temperature for growing (Al,Ga)As top layers for laser structures is discussed controversially in the literature. This is partially due to different growth techniques and regimes used as well as to different annealing procedures applied to the material, but might also be an intrinsic property of this metastable quaternary alloy. Therefore, for understanding this class of semiconductor materials it is essential to correlate structural and electronic investigations.

The unusual band structure of (Ga,In)(N,As) together with the aspect of metastability has a number of implications for studies of (Ga,In)(N,As)-containing heterostructures. As in bulk, structural and electronic investigations need to be combined. Great care has to be taken in comparing results published in the literature on QW structures of nominally similar composition. New $\mathbf{k} \cdot \mathbf{p}$-type models need to be developed for describing the electronic states of such heterostructures.

In the following, the growth and annealing technique related structural properties as well as intrinsic structural properties of the material system will be summarized. It is shown how the metastability of (Ga,In)(N,As) manifests itself in the electronic properties of corresponding heterostructures grown by MBE as well as by MOVPE. It is demonstrated that by careful procedures the alloy can be driven into a stable configuration. It is essential that such a stable configuration exists and can be reliably attained, in order to employ this class of semiconductor alloys in devices.

2. Growth and annealing of diluted nitrides

Due to the metastability of the class of materials under investigation here, growth techniques far from thermodynamical equilibrium have to be applied. The two techniques normally used are MOVPE and MBE. To incorporate nitrogen into the samples, the substrate temperatures of choice are usually low, around 500–550 °C for MOVPE and 400–450 °C in MBE.

Thermal annealing of the samples takes place either *in situ* or *ex situ*. After MOVPE growth, *in situ* annealing is mostly used, where the sample is kept in the reactor under arsenic stabilization for several minutes at about 700 °C. Rapid thermal annealing (RTA) is mainly used after MBE growth of the samples, and takes place *ex situ* at temperatures between 700 and 800 °C for several seconds to a minute, using a second GaAs wafer as a proximity cap. Unstabilized annealing is sometimes applied without arsenic stabilization of the surface in a hydrogen or nitrogen atmosphere at reduced temperatures. There are many reports in the literature on MOVPE and MBE growth of (Ga,In)(N,As) and the incorporation characteristics of N, which is quite different for both techniques (e.g. [28–36]).

3. Structural properties upon growth

It has been shown that the structural properties of the metastable quaternary (Ga,In)(N,As) depend strongly on the N content in the alloy and slightly on the In content. A certain critical N content exists for every In composition, which cannot be exceeded and results in structural degradation of the MQW stack, if one tries to incorporate more N. This critical N content x_c depends slightly on the In concentration of the sample: its value is around 4–5% for solar cell material, having an In content around 8% and drops to around 2–3% for 1.3 μm laser material, where In contents in the range of 30% and higher are required. This morphological phase transition occurs abruptly if the critical N concentration is exceeded and is an intrinsic property of the material, as will be illustrated in the following.

A cross sectional transmission electron microscopic overview picture of an MOVPE grown (Ga,In)(N,As)/GaAs sample containing 12 QWs is shown in figure 1 [37, 38]. The In and N concentration in these layers amounts to 13% and 4%, respectively. The diffraction conditions have been chosen such that the (Ga,In)(N,As) QWs appear with dark contrast compared to the GaAs buffer layers. All the (Ga,In)(N,As)/GaAs periods are well established and the QWs are uniform in thickness. Extended defects caused by strain in the compressively strained material are not observed even in similar samples if the In content is increased to above 30%. For In concentrations higher than 35–40%, depending on growth temperature, the transition to three-dimensional Stranski–Krastanov growth mode takes place in this material system.

Energy-filtering transmission electron microscopy (TEM) has been performed to obtain the elemental distributions across the wells [37]. The Ga and In jump ratio images of an MQW sample containing 30% In and 1.8% N in the wells are depicted in figure 2. It can be seen that there is a Ga deficiency at the position of the QWs, where an increased amount of In is observed. The In is dispersed homogeneously throughout the complete QW and there are no indications of In separation for these samples. From these experiments together with (002) dark field imaging of the QWs it can be concluded that the In distribution is homogeneous throughout the QWs for N concentrations below the critical values. There are scanning tunnelling microscopic investigations of Ga(N,As) samples where an arrangement of N atoms quite consistent with that expected from random occupation is also found with an enhanced occurrence of N nearest-neighbour pairs [39]. Those N nearest-neighbour pairs would certainly not show up in (002) TEM dark field imaging due to their low probability. Several TEM studies of MBE grown samples also reveal no indication for elemental clustering [40].

However, Albrecht *et al* [41] have performed intensive TEM studies on MBE grown (Ga,In)(N,As) QWs and find pronounced lateral fluctuations in (002) dark field images of the QWs, indicating compositional fluctuations, especially for as-grown samples. These compositional fluctuations are attributed to rather large (±5%) fluctuations in the In content throughout the QWs on a length scale of approximately 20 nm, whereas the N content stays constant. These compositional fluctuations, which have also been observed in [42], might be

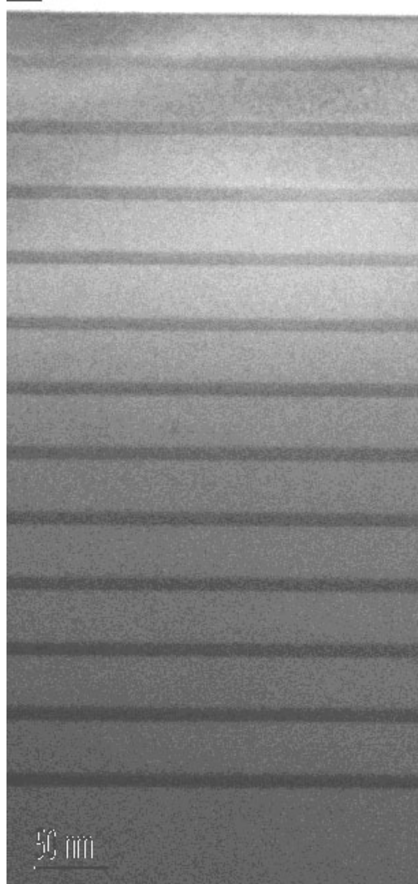

Figure 1. A cross sectional TEM image of an MOVPE grown sample containing 12 $Ga_{0.87}In_{0.13}N_{0.04}As_{0.96}$ QWs separated by GaAs barriers. The diffraction conditions have been chosen such that the (GaIn)(NAs) QWs appear with dark contrast compared to the GaAs layers.

one possible reason for the strong carrier localization in this material system, as this study also shows a constant QW thickness.

Determining the interface roughness of a quaternary material is a rather difficult task. Applying high resolution TEM, high structural quality of the QWs has been confirmed for MOVPE (figure 3) as well as MBE grown [43] samples. It can be shown that—for N contents below the critical value—every QW of the structure exhibits the same roughness at its interfaces. In figure 3, as an example, the second QW of a five times $Ga_{0.78}In_{0.22}N_{0.01}As_{0.99}$/GaAs MQW stack is shown. The interface roughness extends over about 2–5 monolayers at both interfaces.

Bernatz *et al* [44] developed a technique to reveal the interior interfaces of heterostructures as they are formed during growth before cooling down. In this method the surface of interest is covered at growth temperature with a second material. The latter is removed at ambient temperature by highly selective etching procedures. Subsequent atomic force microscopy allows one to study the interface as it was formed during the growth. This provides three-dimensional mapping of interior interfaces on lateral scales of micrometres with lateral resolutions of the order of 10 nm and a vertical resolution of 0.1 nm. This technique has recently been applied to both MOVPE and MBE grown material, and despite the different

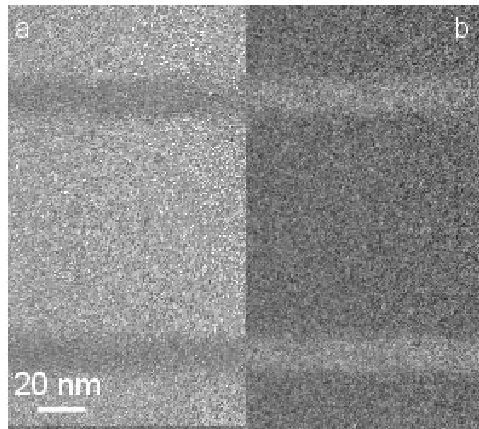

Figure 2. (a) Ga jump ratio image of a $Ga_{0.7}In_{0.3}N_{0.018}As_{0.982}$/GaAs QW sample obtained by energy-filtering TEM. (b) Corresponding In jump ratio image.

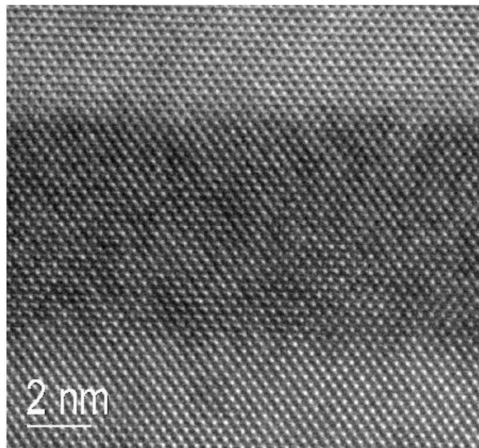

Figure 3. A high resolution TEM image of the second QW of a five times $Ga_{0.78}In_{0.22}N_{0.01}As_{0.99}$/GaAs MQW stack. The interface roughness extends over about 2–5 monolayers at both interfaces.

growth regimes employed by both techniques, striking similarities in the morphology of the interior (Ga,In)(N,As) interface have been demonstrated [45]. The (Ga,In)(N,As) interior interface is rather ragged without any extended features, and a maximum island size of about 10–15 nm and roughnesses between 1 and 2 nm, being in good agreement with what has been concluded from cross sectional TEM images, depending on the growth technique. Monolayer structures cannot be resolved.

Recently, it has been shown by TEM dark field imaging with a combination of strain and composition sensitive reflections that N-induced strain fields in the N-containing ternary and quaternary material exist, although the element distribution is homogeneous [46]. These inhomogeneous strain fields could be caused for example by N–N nearest-neighbour pairs and could have an immense effect on transport and optical properties. The mean distance between the strain fields decreases with increasing N content, being in the range of 10 nm for around 2–3% N material. This value agrees very well with what was reported to be the—unexpectedly short—minority carrier diffusion length in this material [47].

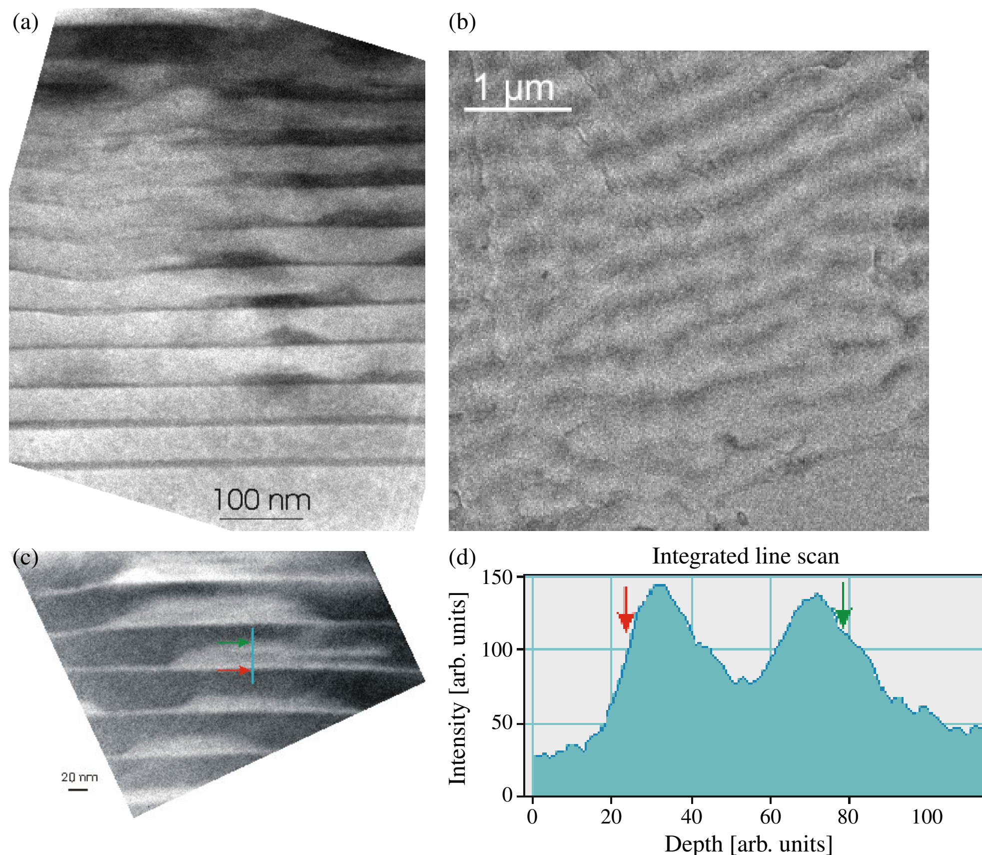

Figure 4. TEM results of a $Ga_{0.87}In_{0.13}N_{0.045}As_{0.955}$/GaAs MQW structure with N content above the critical value: (a) a bright field image taken under identical diffraction conditions as figure 1, (b) a bright field micrograph in plan-view orientation, (c) an In jump ratio image, (d) an integrated linescan over the structure as indicated by the arrows.

(This figure is in colour only in the electronic version)

The nitrogen content in the QWs can be changed by altering the gas partial pressure of the group V precursor substances in MOVPE and is mainly altered by changing the growth rate in MBE. In the following an MQW structure will be discussed which has been formed by reducing the partial pressure of the As precursor (in this case tertiary-butyl-arsine (TBAs)) in MOVPE. This results in an N content of 4.5% under otherwise identical growth conditions as used for the sample depicted in figure 1. Under the conditions applied, a significant deterioration of the MQW structure can be seen (figure 4(a) [37]). The thickness of the wells shows strong modulations in a range of a few monolayers up to 20–22 nm. The thinner parts of the wells are often bent towards the substrate. Starting from the second QW, a strong modulation in the shape of the wells is also observed. Trapezoidal-, dot-, trough- and cusp-like features are seen throughout the wells. The average size of the islands increases with increasing number of wells. This morphological transition can be attributed solely to microscopic strain, as the macroscopic compressive strain of this sample is lower in comparison to that of the one with smooth interface morphologies [37], shown in figure 1. The image contrast throughout the structures, especially, if the rather thick trapezoidal ones are investigated, is not homogeneous

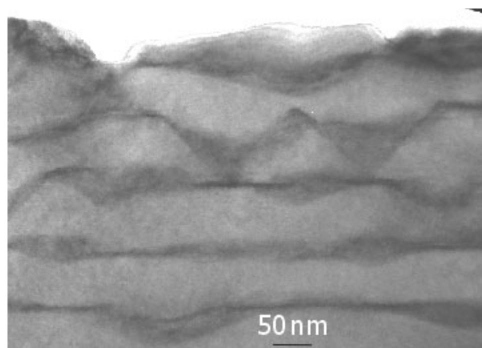

Figure 5. A cross sectional TEM micrograph of an MBE grown (Ga,In)(N,As)/GaAs MQW sample having similar composition as the MOVPE grown sample shown in figure 4.

any more, as has been observed for the sample with lower N content (figure 1). This could be an indication of segregation processes of the elements contained in these wells.

In figure 4(b) a bright field micrograph in plan-view orientation is shown of the same sample as used for figure 4(a). In this micrograph, the geometry and dimensions of the trapezoidal structures can be seen, which are formed with increasing number of wells and which result in modulations of the surface morphology. It becomes obvious that the island formation is actually a two-dimensional phenomenon, resulting in elongated structures, which have approximately the dimensions of several μm times 100–200 nm along two orthogonal $\langle 220\rangle$ directions. A similar kind of anisotropic growth has been observed for mixed III–V alloys on InP [48, 49]. In that case, the anisotropy has been explained with different surface diffusion rates along the [110] and $[1\bar{1}0]$ directions.

Energy-filtering TEM has been carried out to elucidate the Ga and In depth distribution. The In jump ratio images of this sample are shown in figure 4(c), and an integrated linescan over the structure as indicated by the arrows is depicted in figure 4(d). It can be seen that less Ga is incorporated in the trapezoidal structures as well as in the regions in between, which are only a few nm thick. The In concentration profile shows strong inhomogeneities, especially in the thicker regions of the wells. A zone can always be observed directly adjacent to the GaAs/(Ga,In)(N,As) interface, where a very high In fraction is present in the quantum structure. This region is directly followed by one having a lower In content. For the thickest structures, an additional In-rich zone is observed, resulting in a splitting of the wells in up to three zones with different In content. The inhomogeneity of the In distribution is the more astonishing as only the parameters of the group V precursors have been changed compared to the structurally homogeneous sample, and the macroscopic strain has been reduced to yield an almost lattice-matched sample on GaAs.

Hence, the additional nitrogen which is incorporated in this sample has an influence on the In depth distribution. This In segregation in zones with very high In content separated from each other by regions with almost vanishing In concentration has not been observed so far, and could be responsible for the reduction of the macroscopic compressive strain of this sample compared to one having a homogeneous In distribution. Further investigations are in progress in order to clarify this behaviour as well as the preferential growth of the trapezoidal structures along certain crystallographic orientations. These drastic morphological changes are an intrinsic property of the quaternary material system, as they are also observed for MBE grown material of similar composition but grown in a completely different growth-parameter window. Figure 5 depicts a cross sectional TEM micrograph of an MBE grown (Ga,In)(N,As)/GaAs

MQW sample having similar composition as the MOVPE grown one shown in figure 4(a). The structures which can be seen in this micrograph resemble those seen in the previous figure. The QW thickness changes considerably from almost vanishing thickness to about three times the intended thickness. Dot-, trapezoidal-and cusp-like features can also be found in this sample. Investigations into whether the inhomogeneous strain fields reported in [46] and their coalescence might play a role in mediating this structural break down, which seems to be an intrinsic material property up to now, could possibly open up a way of circumventing these structural degradations and incorporating larger amounts of N into the material.

In summary, for appropriate growth conditions, QWs with a high structural quality can be grown by both growth techniques. The roughness of their interfaces to the GaAs barriers is in the range of several monolayers. The presence of phase separation or In accumulation depends strongly on the growth conditions and might limit the performance of the structures already at lower nitrogen contents. One important parameter for both growth techniques is the growth temperature, as shown in [50] for MBE growth. With increasing temperature a transition from smooth two-dimensional growth to three-dimensional growth is observed, which is related to alloy phase-separation [51] and is likely preceded by strong compositional fluctuations that may originate from surface spinoidal decomposition [27]. However, after optimizing the growth conditions, the quaternary metastable material can be grown homogeneously with a high structural perfection. Yet changing the growth parameters to increase the N content in the structures significantly can result in a sudden structural deterioration of the QWs, as soon as the critical nitrogen content is exceeded. A roughening transition from a planar to a three-dimensional island growth is observed, resulting in an inhomogeneous In distribution in the [001] direction as well as in a pronounced thickness modulation across the wells.

4. Changes of structure upon annealing

Thermal annealing is normally used to improve the luminescence properties of (Ga,In)(N,As) structures grown by both techniques, MOVPE and MBE [41, 52–60]. Due to the removal of defects, a significant increase in the PL intensity is observed after annealing, which mostly goes along with a blueshift in the emission wavelength. The magnitude of the blueshift depends on the In and N content in the samples, but is commonly highest for high In and high N contents, and can be as large as 100 meV. Usually, the blueshift is only observed for quaternary (Ga,In)(N,As) and not (or it is much smaller) for the ternary counterparts Ga(N,As) and (Ga,In)As, indicating that it results from the simultaneous presence of In and N in the layer. It is observed irrespective of the growth technique used; however, there might be several mechanisms contributing to an increase of the bandgap of the material. Some of those are growth technique and annealing related, as for example element diffusion on both group III as well as group V sublattices, altering the composition of the structures. Some of the mechanisms are intrinsic for the material systems under investigations, as for example local atomic ordering. The magnitude of the various contributions strongly depends on the growth conditions (e.g. MBE or MOVPE, choice of precursors, N and In concentrations, etc) as well as the annealing conditions (annealing time, ambient, annealing temperature, etc).

There are several reports in the literature dealing with the composition of the quaternary material before and after annealing. Various papers report that the composition of the alloy does not change upon annealing. This is mainly seen by high-resolution x-ray diffraction (XRD) analysis [61, 62]. Tournie *et al* [62] compare XRD patterns of MBE grown samples before and after RTA annealing. Both diffraction patterns show a perfect agreement with each other, demonstrating unambiguously that QW composition and width remain unchanged upon annealing. Figure 6 displays high-resolution XRD patterns and corresponding simulations

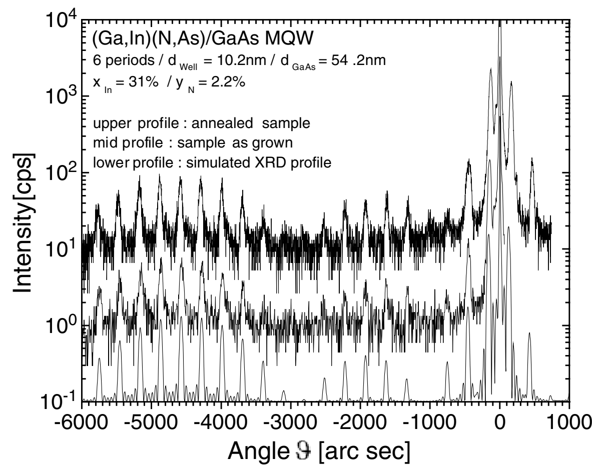

Figure 6. High-resolution XRD patterns and corresponding simulations of MOVPE grown (Ga,In)(N,As)/GaAs MQW samples before and after *in situ* annealing.

for MOVPE grown samples before and after *in situ* annealing [63]. The excellent agreement between the three curves is also obvious here. The distance of the Pendellösung fringes and the width of the QW envelope as well as its position remain unchanged after annealing, indicating no change in thickness of QW and barrier nor a change in composition of the QW upon annealing. Interdiffusion of In into the barriers can also be ruled out from those experiments.

In contrast to that, after different growth and annealing procedures, atomic diffusion on the group III and group V sublattice can take place. It has been presented in [41] that inhomogeneities in the In composition throughout the QWs which have been present after MBE growth can be dissolved upon annealing, resulting in a reduction of the maximum In concentration after annealing. RTA annealing is also shown to result in N diffusion out of the QW. Albrecht *et al* show that the reduction in PL linewidth and in Stokes shift are related to the In distribution homogenization. The blueshift of the PL in these samples is due to a reduced In and N concentration in the QWs upon annealing. Similiar In redistribution effects upon annealing have also been observed by other groups [61, 64].

Strong QW/barrier intermixing (which has been mainly observed for MBE grown samples [52, 54, 57]) can be caused by the enhanced presence of point defects (which originate from the RF nitrogen plasma source used for incorporating N in MBE). Sun *et al* have shown by secondary ion mass spectrometry (SIMS) of MBE samples [65] that intentionally introducing point defects in the material results in the interdiffusion of group III atoms between the QWs and barriers and hence in a blueshift of the PL signal. It is also possible that point defects promote—in addition to interdiffusion—in-plane compositional diffusion.

Several authors even report on a redshift of the PL emission upon RTA of MBE grown samples [66]. Activation of N from interstitial to substitutional sites may be responsible for this redshift. It has been shown by a combination of nuclear-resonance analysis and ion-beam channelling that a significant amount of N is incorporated on interstitial lattice sites during growth [34]. This interstitial N is removed upon annealing. It can be either activated to lattice sites or diffuse out of the sample completely. The authors also observe an outdiffusion of substitutional nitrogen upon RTA which could also explain some of the blueshift of RTA annealed MBE grown samples.

Those studies show that, depending on the growth and annealing conditions used, it is—for both growth and annealing techniques used—possible to keep the QW composition unchanged

or to alter it after annealing. The latter can already introduce a significant blueshift to the PL signal.

An intrinsic contribution to the blueshift is the rearrangement of the local N environment, as it does not alter the macroscopic composition of the crystal. A single (Ga,In)(N,As) crystal with a fixed composition has been shown to possess up to five different bandgaps caused by the five different nearest-neighbour (nn) environments of the N [59]. The N nn environment and hence the bandgap of the material can be tuned by changing the annealing conditions. During growth a Ga-rich environment is favourable for the N as the Ga–N bond is very stable. During annealing, however, the more In-rich environments become preferable as the strain component of the total energy will be lower in these configurations. This nn change presumably takes place on the group V sublattice and is mediated by As vacancies.

There is further proof with structural characterization techniques, like Raman and infrared spectroscopy [60, 61, 67–69], that this hopping of N into In-rich environments upon annealing is indeed one of the processes taking place during the anneal and that it contributes to the blueshift. Changes of the local-vibrational modes of N in (Ga,In)(N,As) in Raman or infrared-absorption spectra are observed. Kurtz *et al* [67] performed infrared spectroscopic measurements on MOVPE grown solar cell material before and after annealing and found that there is mainly a change in the Ga–N stretch mode, which can be explained if the nitrogen environment is converted from NGa_4 to $NInGa_3$. Very convincing evidence for such changes is obtained by Raman spectroscopy close to the E_+ resonance with excitation energies of 2.18 eV [60] and 1.92 eV [68]. It is worth mentioning that under certain growth and annealing conditions there do not seem to be significant changes of the nn environment of N in (Ga,In)(N,As), i.e. the 4Ga environment dominates even after annealing [70].

Recently, near edge x-ray absorption fine structure spectroscopy and extended x-ray absorption fine structure spectroscopy have been undertaken at the N K-edge and the In K-edge respectively for MBE as-grown and annealed samples in tandem with *ab initio* calculations [71]. These measurements indicate a transition from random configuration upon growth to NIn_3Ga upon annealing of the laser material, also minimizing the total energy of the system. Theoretically, the competition between bond and strain energy has also been discussed [23] and a positive order parameter in the sense of a shift towards an In–N bond rich bond distribution has been predicted for thermodynamic equilibrium. These EXAFS data and the theoretical calculations are still discussed controversially in the literature [72], where only a one order of magnitude weaker ordering than predicted in [23] is anticipated.

This compendium of different reports on the miscellaneous reasons for the increase of the bandgap of (Ga,In)(N,As) manifests its metastability as well as the dependence of structural, electronic and optic properties on the growth conditions and novel intrinsic properties as different bandgaps of a material of one single composition.

5. The fine structure of the bandgap

In the following, we will focus on the rearrangement of the local N environment and its influence on the optical properties. In many samples grown by MOVPE or MBE there are indications of changes of the local N environment from a configuration with 4Ga nn to configurations with more In nns (see, for example, [59, 68, 69]).

To reach a better understanding of the effect of the N nn environment on the band structure of $Ga_{1-y}In_yN_xAs_{1-x}$, full sp^3s^* tight-binding supercell calculations have been performed, in which the central group V site was constrained to have a given number m (=0–4) of In nns. In atoms were placed at random on the remaining sites to give the desired overall y. The Hamiltonian was written as $H_1 = H_0 + \Delta H$, where H_0 is the Hamiltonian for (Ga,In)As and ΔH the change due to N incorporation. Pairs of supercells H_0 and H_1 were defined

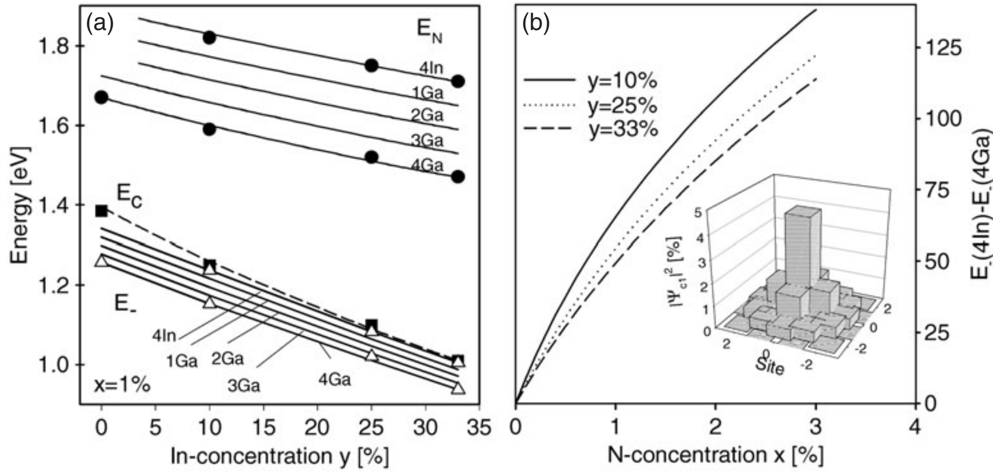

Figure 7. Supercell calculation results of the conduction band structure of $Ga_{1-y}In_yN_xAs_{1-x}$ for various nn environments of the N-centre. (a) y-dependence, constant x. (b) x-dependence, constant y. Inset: the probability density of the conduction band edge wavefunction around the N-centre.

by placing As and N, respectively, onto the central group V site. Calculating separately the wavefunctions ψ_{c0} and ψ_{c1} for H_0 and H_1, one can derive a nitrogen resonant level wavefunction $\psi_N \propto (\psi_{c1} - \langle\psi_{c0}|\psi_{c1}\rangle\psi_{c0})$. This allows one to relate the supercell calculations to the simple level repulsion model by $V_{Nc} = \langle\psi_N|H_1|\psi_{c0}\rangle$, $E_N = \langle\psi_N|H_1|\psi_N\rangle$ and $E_c = \langle\psi_{c0}|H_1|\psi_{c0}\rangle$. Details of the model are given in [17, 25]. These results are corroborated by other theoretical models [23].

Figure 7(a) shows the results of 216-atom supercell calculations (corresponding to $x \approx 1\%$). For each y, the E_N for the five nn configurations are equally spaced with the value for 4Ga nns being always about 220 meV lower than that of 4In nns. Such strong dependence of the energy of isolated, strongly localized impurities on the nn environment is common [73]. Calculations, where the atomic arrangement in the second group III shell and higher shells was altered, only shift E_N by ± 20 meV. This agrees with experiments on Ga(As, P):N where a broadening of 30 meV of the localized N state is observed due to disorder on the group V sublattice [74]. The derived matrix element V_{Nc} linking the N resonant state and the conduction band edge varies between about 2.00 eV $\cdot\, x^{1/2}$ for 4Ga nns to about 1.35 eV $\cdot\, x^{1/2}$ for 4In nns, i.e. the strength of the perturbation of the crystal decreases with increasing number of In nns. The large differences of the five nn environments of N are also reflected in the derived conduction band edge energies E_-. For each y at $x = 1\%$, the E_- values for the five nn configurations are evenly spread over an energy range of about 80 meV below the corresponding unperturbed E_c of (Ga,In)As, with that for 4Ga nns being lowest in energy. The influence of the different nn configurations on the valence band edge is small in comparison to that on the conduction band edge. The magnitude of the splitting $E_-(4Ga) - E_-(4In)$ increases strongly with x for all y in figure 7(b). The three curves were calculated by varying the number of the atoms in the supercell between 1728 ($x \approx 0.1\%$) and 64 ($x \approx 3.1\%$). The inset of figure 7(b) depicts the probability density of the band edge wavefunction ψ_{c1}. About 40% of it is localized around the N impurity and its four nns. Changing the nn configuration of N modifies this localized band-edge wavefunction strongly. Such strong impurity-like band gap behaviour has also been reported for Ga(N,As) [20] and (Ga,In)N [26]. It explains the strong effect of the N impurity environment on the band gap structure of (Ga,In)(N,As).

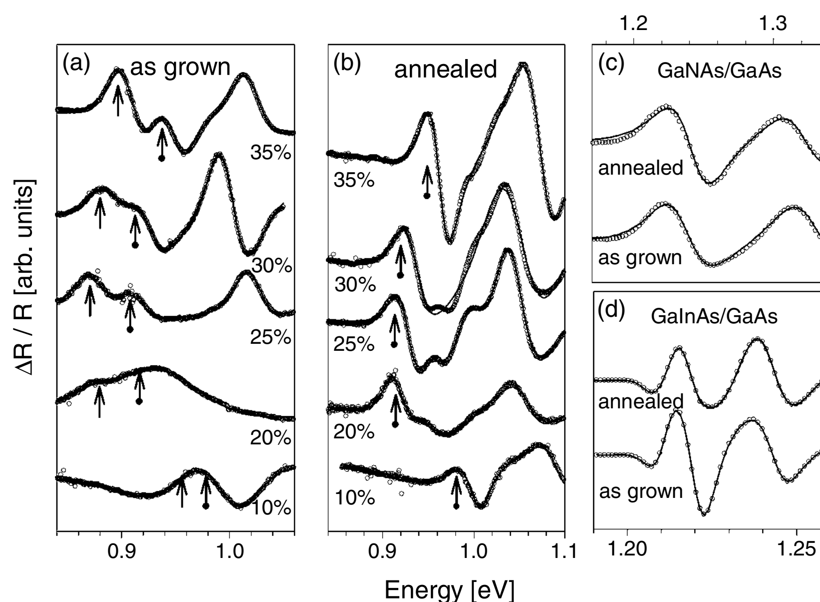

Figure 8. Room-temperature photomodulated reflectance spectra of $Ga_{1-y}In_yN_xAs_{1-x}$/GaAs QWs as-grown and annealed unstabilized at 625 °C (a), (b) $x \approx 2\%$, various y. (c) $x = 1.5\%$, $y = 0\%$. (d) $x = 0\%$, $y = 20\%$.

In the following we want to discuss experimental results concerning the influence of the rearrangement of the nn environment of N on the band structure. The samples studied were $Ga_{1-y}In_yN_xAs_{1-x}$/GaAs QW structures ($y \leqslant 35\%$, $x \leqslant 3\%$, well width ≈8 nm) and $Ga_{1-y}In_yN_xAs_{1-x}$ layers ($y \leqslant 15\%$, $x \leqslant 3\%$) grown by MOVPE. Pieces of the samples were annealed at various temperatures at a constant TBAs partial pressure of 0.0272 mbar for 1 h followed by 25 min either in hydrogen atmosphere (unstabilized) or at the same TBAs partial pressure (As-stabilized). For the annealed samples no indications for a loss of nitrogen in the layers, interdiffusion in the QW structures or phase separation were found by SIMS, TEM or XRD investigations similar to those described in the previous sections.

Figure 8 depicts details of room temperature photomodulated reflectance (PR) spectra of as-grown QW samples and of corresponding samples annealed unstabilized at 625 °C. For the as-grown $Ga_{1-y}In_yN_xAs_{1-x}$/GaAs QWs with $x \approx 2\%$ (figure 8(a)), at energies below 1 eV, a double-peak structure, corresponding to the lowest QW state, develops on increasing y from 10% to 35%. After annealing (figure 8(b)), the peak structure below 1.0 eV has changed: the low-energy signal of the double-peak structure has disappeared for $y \geqslant 0.2$ whereas its high-energy signal has increased in oscillator strength. The energy separation between the two signals of about 30–40 meV is, approximately, independent of y. The disappearance of the low-energy peak in the PR is also reflected in the PL where a shift of the PL band to higher energies occurs. The situation is completely different for the ternary QWs, as depicted in figures 8(c) and (d). Neither for the $GaN_{0.015}As_{0.985}$/GaAs QW nor for the $Ga_{0.8}In_{0.2}As$/GaAs QW are a blueshift or a dramatic change of the PR spectra seen after annealing. This is also confirmed by the room temperature PL spectra, which do not show a blueshift after thermal treatment.

The inset of figure 9(a) shows the dependence of the room temperature PL of a $Ga_{0.7}In_{0.3}N_{0.01}As_{0.99}$/GaAs QW structure recorded after As-stabilized annealing.

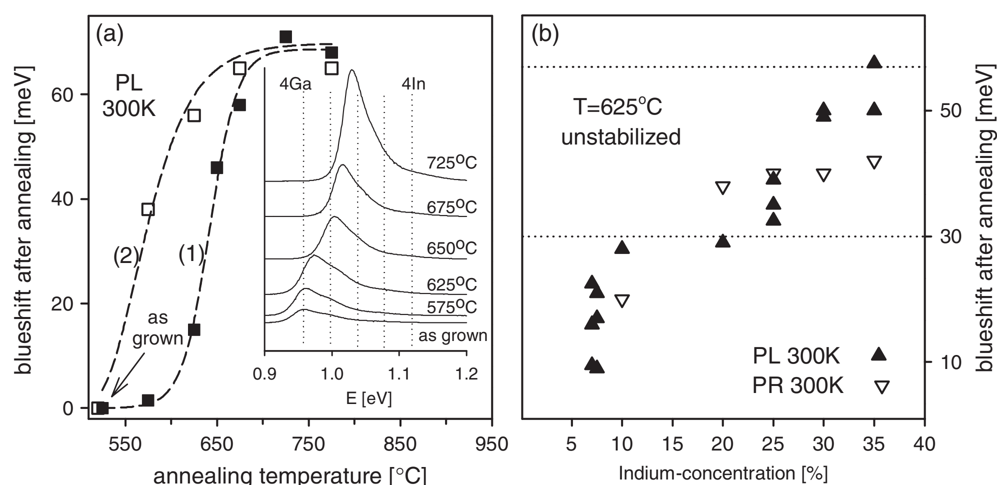

Figure 9. (a) The photoluminescence blueshift of a $Ga_{0.7}In_{0.3}N_{0.01}As_{0.99}$/GaAs QW versus annealing temperature annealed As-stabilized (1) and unstabilized (2). Inset: room-temperature photoluminescence corresponding to (1). (b) The blueshift after unstabilized annealing at 625 °C of $Ga_{1-y}In_yN_xAs_{1-x}$/GaAs QWs ($x \approx 2\%$) versus y.

Apart from the increase of the PL intensity, which is mainly due to a reduction of non-radiative recombination centres during annealing, an unusual blueshift of the PL maximum together with significant changes of the PL line shape are observed. The PL spectra consist of overlapping bands separated by about 30 meV whose relative intensities are changed such that the maximum of the PL is shifted to higher energies. At room temperature, these PL bands must originate from the band–band transitions, which is confirmed by the negligible Stokes shifts between the PL and the PR signals. Therefore, the shift of the maximum of the room temperature PL is also a measure for the redistribution of the combined density of states at the band gap in (Ga,In)(N,As).

The dependence of the blueshift of the PL maximum obtained from the spectra shown in the inset is depicted as curve (1) in figure 9(a). Below a critical annealing temperature T_c of about 600 °C, the band gap remains stable, but for higher temperatures a blueshift is observed which reaches about 70 meV for $T > 700$ °C. Curve (2) has been recorded using pieces of the same $Ga_{0.7}In_{0.3}N_{0.01}As_{0.99}$/GaAs QW structure as before, but unstabilized annealing conditions. The T_c of curve (2) is smaller than that of curve (1) and the blueshift already saturates at lower annealing temperatures.

Figure 9(b) is a plot of blueshifts measured by PL and PR at 300 K for various $Ga_{1-y}In_yN_xAs_{1-x}$/GaAs QWs and $Ga_{1-y}In_yN_xAs_{1-x}$ epitaxial layers with $1\% < x < 2\%$ after unstabilized annealing at 625 °C as a function of y. At $y \approx 7\%$ a step-like increase of the energy shift is observed. After a plateau at about 30 meV, the blueshift increases to about 60 meV as y increases.

The double peak structure for the lowest transition in the $Ga_{1-x}In_xN_yAs_{1-y}$ QWs in the PR spectra (figure 8(a)) as well as the PL line shape changes (figure 9(a)) can be interpreted as a genuine proof of the existence of local band gaps arising from different nn configurations of the N impurity. The dependence of the annealing effect on TBAs partial pressure (figure 9(a)) leads to the conclusion that the change of N environment is enhanced by As vacancies. Thus, the reconfiguration process takes place on the group V sublattice. It probably arises due to a hopping of N ions to more favourable In-rich environments via an As vacancy. Combining the

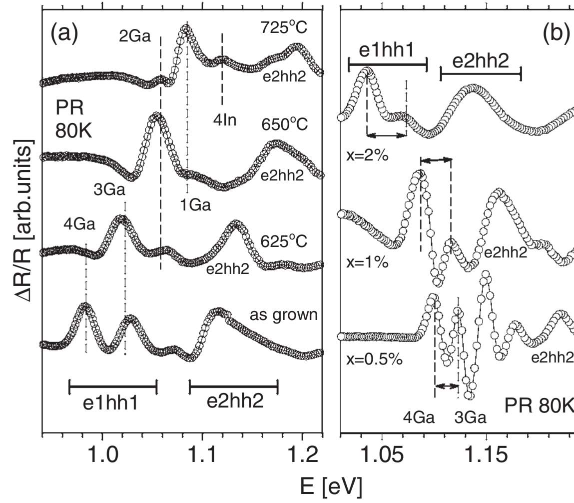

Figure 10. Photomodulated reflectance spectra at 80 K: (a) $Ga_{0.7}In_{0.3}N_{0.01}As_{0.99}$/GaAs QW as-grown and annealed As-stabilized at 625, 650, 750 °C. (b) $Ga_{0.7}In_{0.3}N_xAs_{1-x}$/GaAs QW with $x = 0.5\%$, 1%, 2%.

results of figure 9(b) with ion statistics shows that this hopping process is of very short range and mainly takes place between neighbouring sites. The N-hopping process is driven by the competition between chemical bonding and local strain contributions to the site energies of the different N environments. During the growth process chemical bonding aspects dominate at the surface which favour Ga–N bonds instead of In–N bonds [75]. This surface state is frozen in during the non-equilibrium growth process. In contrast to the surface, In-rich nn configurations of N are favoured in bulk at equilibrium due to the dominance of local strain effects. Therefore, the frozen non-equilibrium bulk state can be transformed into the equilibrium bulk state by annealing under appropriate conditions.

The discrete character of the set of five bands comprising the actual band gap and the x-dependence of the energy separation between the bands is verified by PR at low temperatures. Figure 10(a) depicts PR spectra of four pieces of a $Ga_{0.7}In_{0.3}N_{0.01}As_{0.99}$/GaAs QW as-grown and annealed As-stabilized at 625, 650 and 725 °C, respectively. The e1hh1 and e2hh2 transitions dominate the spectra; forbidden hh-transitions do not contribute significantly. Light-hole transitions do not need to be considered as they are at higher energies due to strain and confinement. The e1hh1 signal shows a distinct fine structure corresponding to the conduction edge states of different N environments, e.g. 4Ga and 3Ga nn environments for the as-grown sample. Throughout the series the energy positions of the five bands hardly change, but with increasing annealing temperature the oscillator strengths of the signals are redistributed such that the In-rich environments become more dominant. This redistribution is also reflected in the line shape of the e2hh2 signal, which consists of overlapping contributions of the five environments. But these are smeared out so that individual signals can no longer be distinguished, similar to the corresponding room temperature PL (see the inset in figure 9(a)). The conduction band edge is characterized by wavefunctions which are strongly localized near the N-centres, leading to large energy separations between the corresponding conduction band edges. The unique phenomenon of inherent order in the frame of disorder is that, despite the alloy disorder, five discrete band gaps corresponding to the five ligand fields exist and are resolvable by modulation spectroscopy.

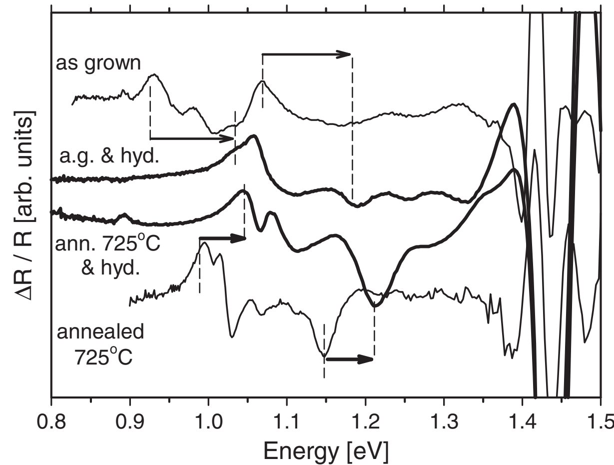

Figure 11. Photomodulated reflectance spectra at 300 K: $Ga_{0.7}In_{0.3}N_{0.01}As_{0.99}$/GaAs QW as-grown and annealed at 725 °C before (thin curves) and after (thick curves) hydrogenation treatment.

Figure 10(b) shows PR spectra of three as-grown $Ga_{0.7}In_{0.3}N_xAs_{1-x}$/GaAs QWs with different $x \approx 0.5\%$, 1% and 2%. In all spectra the e1hh1 signal shows a fine structure originating from the 4Ga and 3Ga nn environments. With increasing x, all the QW states shift to lower energies as expected from the increasing level repulsion effect, but also the energy splitting between the two conduction band edge states due to 4Ga and 3Ga nn environments increases from about 20 meV for $x \approx 0.5\%$ to about 40 meV for $x \approx 2\%$. The corresponding total splittings $E_-(4\text{Ga}) - E_-(4\text{In})$ agree reasonably with the calculated values (figure 7(b)) considering an enhancement at lower temperatures as the band edge E_c approaches the N level E_N.

Further confirmation that the fine structure of the e1hh1 transition observed in these MOVPE grown $Ga_{0.7}In_{0.3}N_xAs_{1-x}$/GaAs QW structures arises due to different N nn environments is given when hydrogenating the samples. It is well established by hydrogenation experiments of Ga(N,As) or (Ga,In)(N,As) based structures that hydrogen almost completely neutralizes the effect of N on the band structure of the GaAs and (Ga,In)As host [76–80].

Figures 11 and 12 depict PR spectra and XRD traces, respectively, of an as-grown piece and a piece annealed at 725 °C under As-stabilized conditions of a $Ga_{0.7}In_{0.3}N_{0.01}As_{0.99}$/GaAs before and after hydrogenation treatment. The similarity of the XRD traces of the as-grown and annealed QW before hydrogenation underlines again, as discussed before, that under these moderate annealing conditions no loss of nitrogen in the layers, no interdiffusion, and no phase separation occur in the QW structures. The PR spectra of the two unhydrogenated samples show the familiar features for the QW ground state transition e1hh1, i.e. after annealing the e1hh1 transition is blueshifted significantly and the double-peak structure disappears. After hydrogenation there is a slight change of the XRD traces observable which can be accounted for by a change of the strain state of the (Ga,In)(N,As) layers due to the formation of N–H complexes [80]. More interesting are the PR spectra of the hydrogenated samples. After hydrogenation, when the effect of N on the band structure is virtually switched off, the ground state transitions of both specimens are further blueshifted such that both transition energies are approximately the same, corresponding to that of the ground-state transition of an N-free QW. This result confirms again that the fine structure of the lowest QW transition arises due to different local N environments, and that the blueshift due to annealing in these samples is almost entirely caused by a rearrangement of the local N environment, i.e. interdiffusion of Ga and In, loss of N, etc play a minor role.

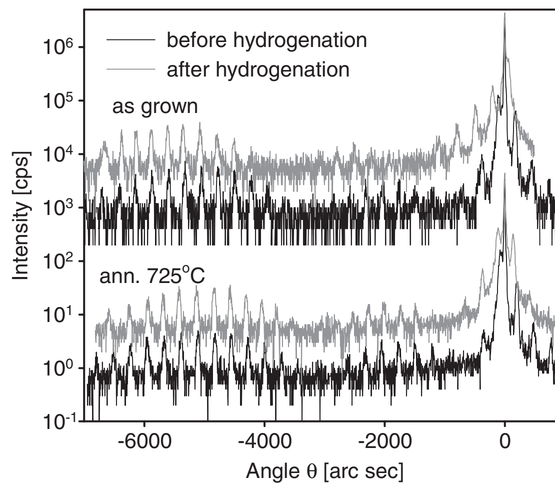

Figure 12. High-resolution XRD traces at 300 K: $Ga_{0.7}In_{0.3}N_{0.01}As_{0.99}$/GaAs QW as-grown and annealed at 725 °C before (black) and after (grey) hydrogenation treatment.

In summary, the band gap of $Ga_{1-y}In_yN_xAs_{1-x}$ depends on the local N environment. Therefore it is not simply a function of composition y and x, but also depends strongly on the material history, e.g. the growth conditions as well as the annealing conditions. This is a strong manifestation of the metastability of this quaternary alloy system.

6. Conclusions

This paper gave an overview of the correlations between structural and electronic properties of (Ga,In)(N,As) based QW structures. The first part of the paper dealt with structural aspects of as-grown samples. The morphological phase transition occurring in $Ga_{1-y}In_yN_xAs_{1-x}$ at a critical N concentration x_c was demonstrated to be an intrinsic property of this material system, independent of the growth method, i.e. MBE or MOVPE. Furthermore it was shown that depending on the growth conditions and the N content, large strain fields are introduced. Great care needs to be taken to obtain smooth interfaces in the structures. Smooth interfaces with interface roughnesses of only a few monolayers were realized. The second part of the paper dealt with the effects of thermal annealing on the structural and electronic properties of (Ga,In)(N,As). Heterostructures containing quaternary (Ga,In)(N,As), in contrast to structures based on ternary Ga(N,As), are metastable and therefore the structure of the electronic states depends on the sample history. In particular, we discuss different mechanisms contributing to a blueshift of the band gap on annealing. One clearly has to distinguish between extrinsic and intrinsic contributions. Of the latter, we discuss the fine structure of the (Ga,In)(N,As) band gap in detail and establish the strong correlation between the actual band gap and the dominating nearest-neighbour configuration of the N atoms in the quaternary alloy. Despite the complexity of the problem it appears that by thermal annealing a stable electronic configuration might be achieved which seems reproducible and within limits independent of the growth method, i.e. MBE or MOVPE. However, further detailed studies are required to confirm this. Of course, the existence of such a stable electronic configuration is the fundamental prerequisite for any theoretical description or parameterization of the electronic band structure of these alloys. This prerequisite can be considered fulfilled for heterostructures based on ternary Ga(N,As) such as Ga(N,As)/GaAs QWs and (Ga,In)As/Ga(N,As) QWs.

Acknowledgments

We would like to thank all our collaborators of the DFG-Forschergruppe 'Metastable Compound Semiconductors and Heterostructures' in Marburg as well as our external collaborators at the University of Rome, NMRC Cork, Daresbury Laboratories, and University of Surrey. We would especially like to thank Wolfgang Stolz and Wolfram Heimbrodt (Philipps-University Marburg) and James S Harris (Stanford University, USA) and their groups for fruitful discussion and for conceding several figures before publication. We are also very grateful for financial support by the DFG, BMBF, the Alexander von Humboldt foundation and the European Community.

References

[1] Makimoto T, Saito H, Nishida T and Kobayashi N 1997 *Appl. Phys. Lett.* **70** 2984
[2] Weyers M, Sato M and Ando H 1992 *Japan. J. Appl. Phys.* **31** L853
[3] Kondow M, Uomi K, Hosomi K and Mozume T 1994 *Japan. J. Appl. Phys.* **33** L1056
[4] Pozina G, Ivanov I, Monemar B, Thordson J V and Andersson T G 1998 *J. Appl. Phys.* **84** 3830
[5] Bi W G and Tu C W 1997 *Appl. Phys. Lett.* **70** 1608
[6] Grüning H, Chen L, Hartmann Th, Klar P J, Heimbrodt W, Höhnsdorf F, Koch J and Stolz W 1999 *Phys. Status Solidi* b **215** 39
[7] Perkins J D, Mascarenhas A, Zhang Y, Geisz J F, Friedman D J, Olson J M and Kurtz S R 1999 *Phys. Rev. Lett.* **82** 3312
[8] Klar P J, Grüning H, Heimbrodt W, Koch J, Höhnsdorf F, Stolz W, Vicente P M A and Camassel J 2000 *Appl. Phys. Lett.* **76** 3439
[9] Shan W, Walukiewicz W, Ager J W III, Haller E E, Geisz J F, Friedman D J, Olson J M and Kurtz S R 1999 *Phys. Rev. Lett.* **82** 1221
[10] Perkins J D, Mascarenhas A, Geisz J F and Friedman D J 2001 *Phys. Rev.* B **64** 121301(R)
[11] Kent P R C and Zunger A 2001 *Phys. Rev.* B **64** 115208
[12] Kent P R C and Zunger A 2001 *Phys. Rev. Lett.* **86** 2613
[13] Gonzalez Szwacki N and Boguslawski P 2001 *Phys. Rev.* B **64** 161201(R)
[14] Lindsay A and O'Reilly E P 2001 *Solid State Commun.* **118** 313
[15] Jones E D, Modine N A, Allerman A A, Kurtz S R, Wright A F, Tozer S T and Wei X 1999 *Phys. Rev.* B **60** 4430
[16] Mattila T, Wei S-H and Zunger A 1999 *Phys. Rev.* B **60** R11245
[17] Lindsay A and O'Reilly E P 1999 *Solid State Commun.* **112** 443
[18] Bellaiche L, Wei S-H and Zunger A 1997 *Appl. Phys. Lett.* **70** 3558
[19] Bellaiche L, Wei S-H and Zunger A 1996 *Phys. Rev.* B **54** 17568
[20] Wei S-H and Zunger A 1996 *Phys. Rev. Lett.* **76** 664
[21] Rubio A and Cohen M L 1995 *Phys. Rev.* B **51** 4343
[22] Neugebauer J and Van de Walle C G 1995 *Phys. Rev.* B **51** 10568
[23] Kim K and Zunger A 2001 *Phys. Rev. Lett.* **86** 2609
[24] Kent P R C, Bellaiche L and Zunger A 2002 *Semicond. Sci. Technol.* **17** 851
[25] O'Reilly E P, Lindsay A, Tomić S and Kamal-Saadi M 2002 *Semicond. Sci. Technol.* **17** 870
[26] Bellaiche L and Zunger A 1998 *Phys. Rev.* B **57** 4425
[27] Asomoza R, Elyukhin V A and Pena-Sierra R 2002 *Appl. Phys. Lett.* **81** 1785
[28] Pan Z, Miyamoto T, Schlenker D, Sato S, Koyama F and Iga K 1998 *J. Appl. Phys.* **84** 6409
[29] Xin H P and Tu C W 1998 *Appl. Phys. Lett.* **72** 2442
[30] Höhnsdorf F, Koch J, Agert C and Stolz W 1998 *J. Cryst. Growth* **195** 391
[31] Harmand J C, Ungaro G, Largeau L and Le Roux G 2000 *Appl. Phys. Lett.* **77** 2482
[32] Egorov A Yu *et al* 2001 *J. Cryst. Growth* **227/228** 545
[33] Pan Z, Li L, Zhang W, Wang X, Lin Y and Wu R 2001 *J. Cryst. Growth* **227/228** 516
[34] Spruytte S G, Larson M C, Wampler W, Coldren C W, Petersen H E and Harris J S 2001 *J. Cryst. Growth* **227/228** 506
[35] Kondow M and Kitani T 2002 *Semicond. Sci. Technol.* **17** 746
[36] Kitatani T, Kondow M and Tanaka T 2001 *J. Cryst. Growth* **227/228** 521

[37] Volz K, Hasse A, Schaper A K, Weirich T E, Höhnsdorf F, Koch J and Stolz W 2000 *Mater. Res. Soc. Symp. Proc.* **618** 291
[38] Höhnsdorf F, Koch J, Hasse A, Volz K, Schaper A, Stolz W, Giannini C and Tapfer L 2000 *Physica* E **8** 205
[39] McKay H A, Feenstra R M, Schmidtling T and Pohl U W 2001 *Appl. Phys. Lett.* **78** 82
[40] Harmand J C, Ungaro G, Ramos J, Rao E V K, Saint-Girons G, Tessier R, LeRoux G, Largeau L and Patriarche G 2001 *J. Cryst. Growth* **227/228** 553
[41] Albrecht M, Grillo V, Remmele T, Strunk H P, Egorov A Yu, Dumitras Gh, Riechert H, Kaschner A, Heitz R and Hoffmann A 2002 *Appl. Phys. Lett.* **81** 2719
[42] Pinault M A and Tournie E 2001 *Appl. Phys. Lett.* **78** 1562
[43] Kondow M, Kitatani T, Larson M C, Nakahara K, Uomi K and Inoue H 1998 *J. Cryst. Growth* **188** 255
[44] Bernatz G, Nau S, Rettig R, Jänsch H and Stolz W 1999 *J. Appl. Phys.* **86** 6752
[45] Torunski T *et al* 2004 *J. Cryst. Growth* submitted
[46] Volz K, Torunski T and Stolz W 2004 *J. Appl. Phys.* submitted
[47] Friedman D J, Geisz J F, Kurtz S R and Olson J M 1998 *J. Cryst. Growth* **195** 409
[48] Okada T, Weatherly G C and McComb D W 1997 *J. Appl. Phys.* **81** 2185
[49] Norman A G *et al* 1998 *Appl. Phys. Lett.* **73** 1844
[50] Hierro A, Ulloa J M, Chaveau J M, Trampert A, Pinault M A, Tournie E, Guzman A, Sanchez-Rojas J L and Calleja E 2003 *J. Appl. Phys.* **94** 2319
[51] Pinault M A and Tournie E 2001 *Appl. Phys. Lett.* **79** 3404
[52] Pan Z, Li L H, Zhang W, Lin Y W, Wu R H and Ge W 2000 *Appl. Phys. Lett.* **77** 1280
[53] Francoeur S, Sivaraman G, Qiu Y, Nikishin S and Temkin H 1998 *Appl. Phys. Lett.* **72** 1857
[54] Buyanova I A, Pozina G, Hai P N, Thing N Q, Bergman J P, Chen W M, Xin H P and Tu C W 2000 *Appl. Phys. Lett.* **77** 2325
[55] Kitatani T, Nakahara K, Kondow M, Uomi K and Tanaka T 2000 *J. Cryst. Growth* **209** 345
[56] Gilet P, Chenevas-Paule A, Duvaut P, Grenouillet L, Hollinger P, Million A, Rolland G and Vannuffel C 1999 *Phys. Status Solidi* a **176** 279
[57] Xin H P, Tu C W and Geva M 1999 *Appl. Phys. Lett.* **74** 2337
[58] Kageyama T, Miyamoto T, Makino S, Koyama F and Iga K 1999 *Japan. J. Appl. Phys.* **38** L298
[59] Klar P J, Grüning H, Koch J, Schäfer S, Volz K, Stolz W, Heimbrodt W, Kamal Saadi A M, Lindsay A and O'Reilly E P 2001 *Phys. Rev.* B **64** 121203(R)
[60] Wagner J, Geppert T, Köhler K, Ganser P and Maier M 2003 *Solid-State Electron.* **47** 461
[61] Pavelescu E M, Jouhti T, Dumitrescu M, Klar P J, Karirinne S, Fedorenko Y and Pessa M 2003 *Appl. Phys. Lett.* **83** 1497
[62] Tournie E, Pinault M A, Laugt M, Chaveau J M, Trampert A and Ploog K H 2003 *Appl. Phys. Lett.* **82** 1845
[63] Koch J, Volz K, Kunert B, Torunski T and Stolz W 2004 at press
[64] Kudrawiec R, Sek G, Misiewicz J, Gollub D and Forchel A 2003 *Appl. Phys. Lett.* **83** 2772
[65] Sun H D, Macaluso R, Dawson M D, Robert F, Bryce A C, Marsh J H and Riechert H 2003 *J. Appl. Phys.* **94** 1550
[66] Yang X, Heroux J B, Jurkovic M J and Wang W I 1999 *J. Vac. Sci. Technol.* B **17** 1144
[67] Kurtz S, Webb J, Gedvilas L, Friedman D, Geisz J, Olson J, King R, Joslin D and Karam N 2001 *Appl. Phys. Lett.* **78** 748
[68] Wagner J, Geppert T, Köhler K, Ganser P and Herres N 2001 *J. Appl. Phys.* **90** 5027
[69] Kitatani T, Kondow M and Kudo M 2001 *Japan. J. Appl. Phys.* 2 **40** L750
[70] Alt H Ch, Egorov A Yu, Riechert H, Wiedemann B, Meyer J D, Michelmann R W and Bethge K 2001 *Physica* B **302/303** 282
[71] Lordi V, Gambin V, Friedrich S, Funk T, Takizawa T, Uno K and Harris J S 2003 *Phys. Rev. Lett.* **90** 145505
[72] Ciatto G *et al* 2003 *Phys. Rev.* B **68** 161201
[73] Samuelson L, Nilsson S, Wang Z-G and Grimmeiss H M 1984 *Phys. Rev. Lett.* **53** 1501
[74] Mariette H, Chevallier J and Leroux-Hugon P 1980 *Phys. Rev.* B **21** 5706
[75] Matsuoka T, Sasaki T and Katsui A 1990 *Optoelectron. Devices Technol.* **5** 53
[76] Amore Bonapasta A, Filippone F, Giannozzi P, Capizzi M and Polimeni A 2002 *Phys. Rev. Lett.* **89** 216401
[77] Polimeni A, Baldassarri Höger von Högersthal G, Bissiri M, Capizzi M, Fischer M, Reinhardt M and Forchel A 2001 *Phys. Rev.* B **63** 201304(R)
[78] Baldassarri Höger von Högersthal G, Bissiri M, Polimeni A, Capizzi M, Fischer M, Reinhardt M and Forchel A 2001 *Appl. Phys. Lett.* **78** 3472
[79] Capizzi M *et al* 2003 *Mater. Res. Soc. Symp. Proc.* **719** 251
[80] Klar P J, Grüning H, Güngerich M, Heimbrodt W, Koch J, Torunski T, Stolz W, Polimeni A and Capizzi M 2003 *Phys. Rev.* B **67** 121206(R)